STIC-ILL

Q1. N2
TMC

From: Schmidt, Mary
Sent: Thursday, May 16, 2002 2:41 PM
T : STIC-ILL
Subject: references, 09/646,825

please locate the following:

1. Bau et al, NAR 22:2811-2816 (1994)
2. Dean et al., NAR 14:2229-2240 (1986)
3. Malter et al, Science 246:664-666 (1989)
4. Shaw et al., Cell 46:659-667 (1986)
5. van Aarsen et al., Plant mol. biol. 28:513-524 (1995)
6. Wilson et al., Nature336:396-399 (1998).

1988

Thanks,
Melissa
11D05
11th floor mailbox

Removal of poly(A) and consequent degradation of c-*fos* mRNA facilitated by 3′ AU-rich sequences

Tim Wilson & Richard Treisman*

MRC Laboratory of Molecular Biology, MRC Centre, Hills Road, Cambridge CB2 2QH, UK

The c-*fos* proto-oncogene provides a good system to study the processes underlying messenger RNA degradation. After growth factor stimulation of susceptible cells, the c-*fos* transcription rate transiently increases from a low basal level by as much as 50-fold[1], producing a large amount of exceedingly unstable c-*fos* mRNA that is rapidly degraded[1-3]. Here, we investigate the c-*fos* mRNA degradation process, and find that: (1) ongoing translation of the c-*fos* mRNA itself is required for its degradation; (2) after synthesis, the mRNA poly(A) tail is rapidly removed, in a translation-dependent manner, leading to accumulation of apparently de-adenylated RNA; (3) deletion or replacement of an AU-rich sequence at the mRNA 3′ end significantly stabilizes the mRNA; (4) deletion of the 3′ AU-rich sequences dramatically slows the poly(A) shortening rate. These results suggest that the 3′ AU-rich sequences act to destabilize the mRNA by directing rapid removal of the mRNA poly(A) tract.

In mouse NIH3T3 cells, c-*fos* mRNA accumulates to high levels by 30 min after serum stimulation, and decays to pre-stimulation levels after 90 min (Fig. 1, lanes 1-6). We used an actinomycin D chase to examine mRNA decay in the absence of continuing transcription. Control experiments showed that addition of actinomycin together with serum is sufficient to block transcription induction completely, demonstrating that the inhibitor acts virtually instantaneously (data not shown). Actinomycin treatment slightly inhibits c-*fos* mRNA turnover (Fig. 1, compare lanes 1-6 with 7-12). When cells are stimulated with serum in the presence of cycloheximide, c-*fos* mRNA is completely stable for at least 90 minutes after actinomycin D addition (Fig. 1, compare lanes 13-15 with 9-12). To test whether cycloheximide acts instantaneously, we added the inhibitor 30 min after serum stimulation and measured RNA levels at later times. Little, if any, degradation was subsequently observed, indicating that cycloheximide acts instantly to block mRNA turnover. Similar results were obtained with c-*fos* mRNA transcribed from the endogenous HeLa cell c-*fos* gene (data not shown). These results are consistent with the notion that turnover of c-*fos* mRNA is sensitive to the inhibition of protein synthesis because it requires ongoing translation of the c-*fos* mRNA itself, rather than continuous synthesis of a labile degradative protein.

Previous work has shown that c-*fos* RNA changes in length before turnover: it has been suggested that this may be due to poly(A) tail shortening[4,5]. To test this idea, we used a non-denaturing gel assay to analyse HeLa cell c-*fos* transcripts. An RNA probe continuously radiolabeled with ^{32}P, spanning the mRNA 3′ end was annealed to total cell RNA, the resulting duplexes were treated with nuclease T1, and the nuclease-resistant RNA was fractionated by non-denaturing or denaturing gel electrophoresis. Under the conditions used, the poly(A) remains intact and is not cleaved from the mRNA. Upon non-denaturing gel electrophoresis, the mixed single-strand/duplex RNA will migrate with mobility dependent on poly(A) tail length; heterogeneity in poly(A) length will cause migration as a smear rather than a sharp band. The results are shown in Fig. 2. HeLa cells have a somewhat higher basal level of c-*fos* transcription than the 3T3 cells discussed above, but the characteristic transient accumulation of c-*fos* mRNA still occurs after serum stimulation (Fig. 2*a*, lanes 1-6, lower panel). At early times after

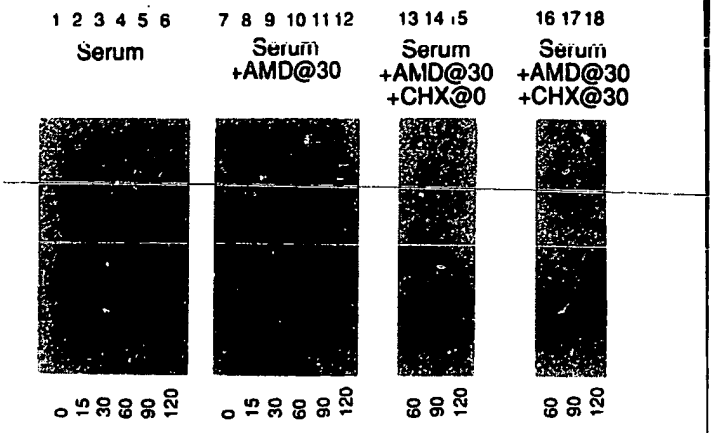

Fig. 1 Translation of c-*fos* mRNA is required for its degradation. Serum-starved NIH3T3 cells were stimulated as indicated. Total cellular RNA was prepared at the times indicated after stimulation and 30 μg analysed for murine c-*fos* mRNA (c-*fos*^{M}) by ribonuclease protection mapping. Lanes 1-6, RNA from cells at 0, 15, 30, 60, 90 and 120 min after stimulation with 15% fetal calf serum. Lanes 7-13, as lanes 1-6 but with 5 μg ml^{-1} actinomycin D (AMD) added 30 min after stimulation. Lanes 13-15, RNA at 60, 90 and 120 min after stimulation with serum and 10 μg ml^{-1} cycloheximide (CHX); 5 μg ml^{-1} actinomycin D was added 30 min after serum stimulation. Lanes 16-18, RNA at 60, 90 and 120 min after serum stimulation, with both actinomycin D and cycloheximide added 30 min after stimulation.

Methods. Total cell RNA preparation and RNAse mapping were as previously described[4]. The probe was generated from plasmid pSP64F^{M}5′, which carried an *Aha*II fragment (nucleotides −14 to +180) spanning the 5′ end of the murine c-*fos* gene (c-*fos*^{M}; ref. 29) inserted in the antisense orientation in the *Eco*RI site of pSP64. Correctly initiated c-*fos*^{M} RNA generates a 180-nucleotide RNAse-resistant fragment from this probe.

stimulation most c-*fos* mRNA molecules carry a long poly(A) tail (Fig. 2*a*, lanes 2, 3); later, the poly(A) length distribution becomes more heterogeneous (Fig. 2*a*, compare lanes 2, 3 with 5, 6). At 40-45 min after stimulation, the majority of HeLa cell c-*fos*^{H} (human c-*fos*) RNA molecules carry only short poly(A) tracts or are de-adenylated (Fig. 2*a*, lanes 5, 6). Control experiments showed that the smears observed were due to poly(A), as pretreatment of the RNA with RNAse H in the presence of oligo(dT) led to the generation of hybrids of the length predicted for those generated by de-adenylated c-*fos*^{H} RNA (data not shown). To establish a precursor-product relationship between the polyadenylated and de-adenylated c-*fos*^{H} mRNA, we performed an actinomycin D chase at 15 min after stimulation, a time at which most RNA has a long poly(A) tail (Fig. 2*a*, lanes 10-16). This experiment confirms that the apparent change in poly(A) length is due to shortening of initially long chains rather than *de novo* synthesis of shorter molecules. In addition, the results suggest that the mRNA is stable until the poly(A) tail has been substantially removed, after which the RNA is degraded (Fig. 2*a*, lanes 2, 10-16). In the case of c-*myc* RNA degradation *in vitro*, cleavage within an AU-rich region has been reported[6]; however, we did not detect increased cleavage within the c-*fos* AU-rich region during mRNA degradation (data not shown). Rapid poly(A) shortening requires ongoing translation, as serum stimulation in the presence of cycloheximide results in a greatly decreased shortening rate (Fig. 2*b*, lanes 1-3). Although shortening is observed at later times, this may reflect the toxic effects of the drug.

To examine regions of the c-*fos* mRNA involved in mRNA degradation, we concentrated on the 811-nucleotide long 3′ untranslated region. The c-*fos* 3′ sequences are required for

* To whom correspondence should be addressed: Imperial Cancer Research Fund, PO Box 123, Lincoln's Inn Fields, London WC2A 3PX, UK.

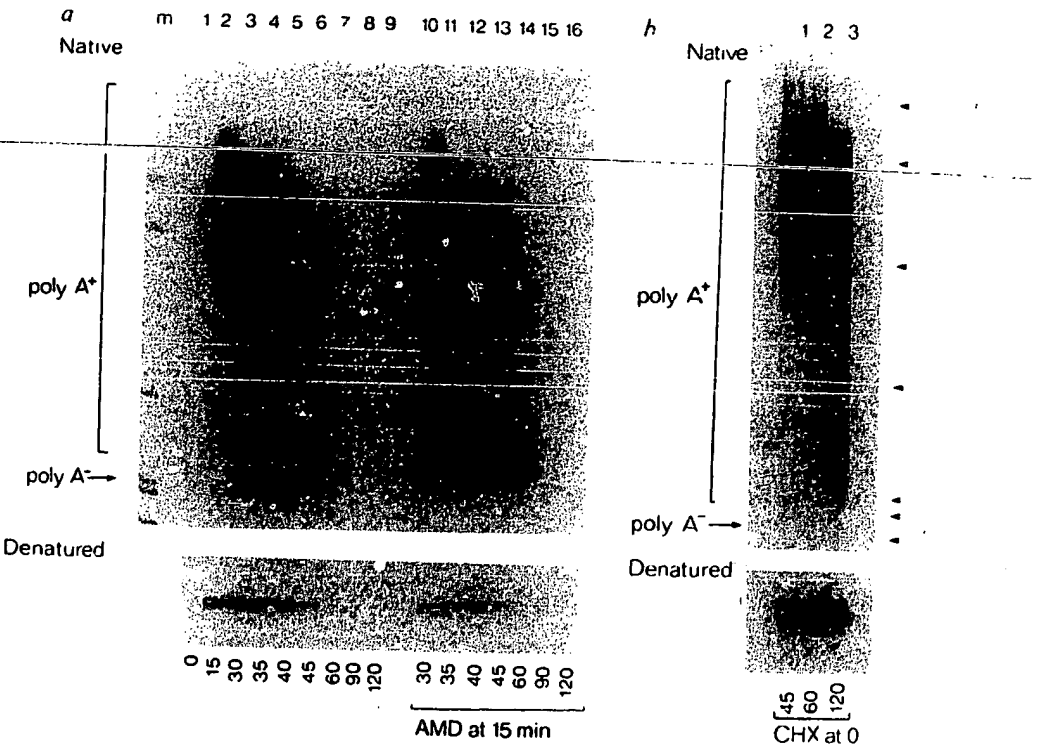

Fig. 2 Analysis of c-*fos*^{H} poly(A) shortening rates. RNAse T1-resistant hybrids formed between c-*fos*^{H} RNA and a probe spanning the 3' end of the mRNA were fractionated on non-denaturing (upper panel) or denaturing (lower panel) gels. Times in minutes after stimulation are shown below each lane. *a*, Poly(A) shortening in HeLa cells after serum stimulation. Lanes 1–9, RNA from cells stimulated with serum; lanes 10–16, RNA from serum-treated cells after addition of actinomycin D 15 min after stimulation. *b*, Effect of cycloheximide on poly(A) shortening rate. Lanes 1–3, RNA from cells stimulated with 15% serum and 10 μg ml^{-1} cycloheximide. Arrowheads show positions of pBR322 MspI marker fragments.

Methods. Total cell RNA preparation and RNAse protection mapping were performed as described[4], except that 0.5 μg ml^{-1} RNAse T1 only was used for ribonuclease treatments. The 3' probe plasmid, pSP64 F^{H}3', contains c-*fos*^{H} nucleotides 3,131 (*Nco*I) to ~4,350 (*Aha*III) inserted in the antisense orientation into pSP64. Probe produced from this plasmid linearized at the *Bcl*I site generates a 240-nucleotide fragment mapping the 3' polyadenylation site. Soon after stimulation large amounts of presumptive c-*fos*^{H} mRNA precursor are present that generate fragments complementary to the entire probe (data not shown).

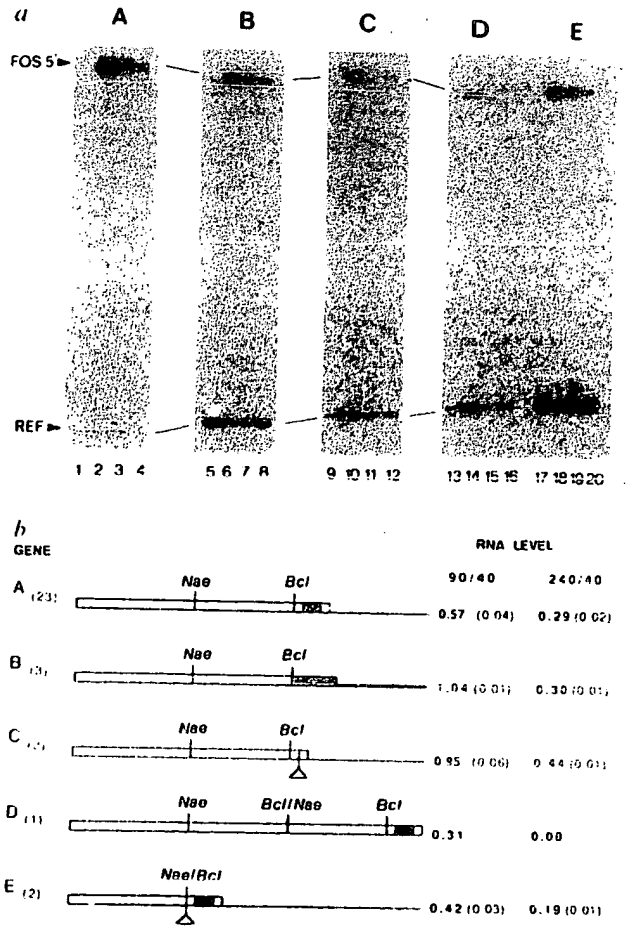

Fig. 3 *a*, Stability of mutant c-*fos*^{H} mRNAs in transient serum stimulation assays for genes A–E. Total cell RNA from cells transfected with the following c-*fos*^{H} plasmids was analysed by RNase protection mapping: lanes 1–4, pF711 (ref. 4); lanes 5–8, pF711.BSVA; lanes 9–12, pF711.ΔAU; lanes 13–16, pF711.13; lanes 17–20, pF711.1223. Each set of lanes contains RNA prepared at 0, 40, 90 and 240 min after serum stimulation. Protected fragments generated by the c-*fos*^{H} and reference α-globin (ref) 5' exons are indicated. *b*, Structures of the genes analysed, c-*fos* 3' AT-rich sequences shown as a solid bar and SV40 sequences cross-hatched; quantitation data, expressed as the ratio of c-*fos*^{H} RNA present at 90 and 240 min after stimulation relative to the peak value at 40 min, are shown at the right, with standard error of the mean in brackets. The number of independent determinations is shown in brackets at the left.

Methods. Cell transfection, RNA preparation, RNAse mapping were as previously described[4]. Plasmids were derived from pF711 (ref. 4) and are as follows. pF711.BSVA has c-*fos*^{H} (ref. 30) sequences 3' to the *Bcl*I site at nucleotide 3,897 replaced by the early region poly(A) addition signal (*Bam*HI+*Bcl*I fragment, nucleotides 2,771 to 2,534). pF711ΔAU lacks c-*fos*^{H} AU sequences (5' 3,949 TGAAAACGTTTTATTGTGTTTTTAATTTATTTATT AAGATGGATTCTCAGATATTTATATTTTTATTTTATTTTTT 4,024 3') and was constructed by site-directed mutagenesis of an appropriate M13 clone using the mutagenic primer 5' CAA⌐GACC TCAAGGTAGATCTGGAAAACTGTTAATGTC 3', which inserts the nucleotides GA at the deletion site. pF711.13 lacks c-*fos*^{H} nucleotides 3,354 (*Nae*I) to 3,897 (*Bcl*I) and contains an insertion of CATG to create an *Nco*I site at the deletion point. pF711.1223 is derived from pF711.13 and contains a duplication of c-*fos*^{H} nucleotides 3,354 to 3,897. The reference plasmid was πSVHSα1?3 (ref. 4). Data were quantitated by densitometric scanning of suitable autoradiograms using the MRC densiometry facility and c-*fos*^{H} RNA values normalized with respect to the α-globin reference standard.

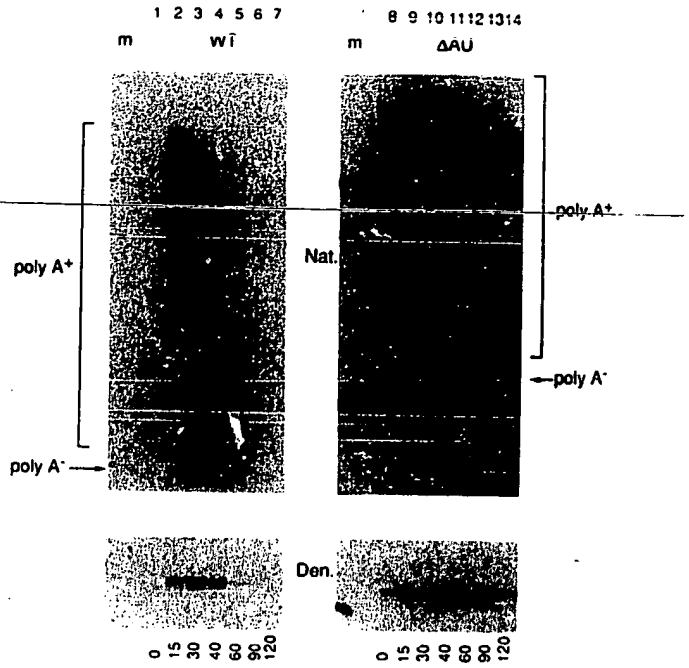

Fig. 4 Analysis of c-*fos*^{H} 3′ poly(A) shortening in transfected NIH3T3 cell pools. RNAse T1 resistant hybrids formed between c-*fos*^{H} RNA and appropriate probes spanning the 3′ end of the mRNAs were fractionated on non-denaturing (upper panel) or denaturing (lower panel) gels. Times in minutes after stimulation are shown below each lane. Pools of cells transfected with either pF711 (WT, lanes 1–7) or pF711ΔAU (lanes 8–14) were serum-starved and restimulated with medium containing 15% FCS.
Methods. NIH3T3 cells were transfected with 1 μg supercoiled c-*fos*^{H} plasmid, 1 μg pSV2neo and 20 μg pUC12 carrier DNA per 75-cm^2 flask using calcium phosphate co-precipitation as described[31]. Colonies of cells resisting 400 μg ml^{-1} G418 were pooled and used for RNA analysis. Southern blotting analysis demonstrated that the pools contained insertions of the transfected genes at many different locations (data not shown). A 3′ probe plasmid, pSP64F^{H}3′ΔAU, analogous to pSP64F^{H}3′, but linearized at the *Pvu*II site, was used to analyse transcripts of the mutant gene. De-adenylated mRNA generates protected fragments of lengths 240 nucleotides and 334 nucleotides from wild-type and mutant genes respectively. RNA preparation and mapping were performed as described in the legend to Fig. 2.

transient c-*fos* mRNA accumulation after serum stimulation, at least in part because they destabilize c-*fos* mRNA[4,7,8]. Previous studies have shown that this region contains a 67-nucleotide AT-rich segment that acts to suppress the transforming activity of the c-*fos* gene[9,10]; this region is highly conserved and is homologous to sequences in the granulocyte/macrophage colony stimulating factor mRNA that confer instability on rabbit β-globin mRNA[11]. Studies of histone mRNA degradation have suggested that degradation is dependent on 3′ untranslated region length[12]. We therefore examined the behaviour of transfected normal and mutant c-*fos*^{H} genes in a transient serum stimulation assay[4]. Mouse NIH3T3 fibroblasts were transfected with c-*fos*^{H} gene plasmids together with a plasmid carrying the human α-globin gene as an internal reference standard. Following RNAse protection analysis, RNA was quantitated by densitometry and c-*fos*^{H} RNA levels were normalized to the α-globin reference signal. In this assay, the peak of wild-type c-*fos*^{H} mRNA accumulation is broader than that of the endogenous gene, reaching a peak at 40 min after stimulation and declining substantially over the next three hours (see Fig. 3, gene A; lanes 1–4; ref. 4). These slower kinetics of mRNA turnover are probably due to the large numbers of template molecules in each transfected cell, as the c-*fos*^{H} genes in stably transfected mouse NIH3T3 cell lines exhibit similar turnover kinetics to the endogenous mouse gene (see below); nevertheless, mutant phenotypes are clearly discernible in the transient assay. When the extreme 3′ end of c-*fos* gene, which contains the AU-rich region, is removed and replaced with the SV40 early region polyadenylation signal mRNA decay is retarded (Fig. 3, gene B: compare lanes 5–8 with 1–4; quantitation in Fig. 3). We used oligonucleotide-directed mutagenesis to construct a gene lacking the AT-rich region (pF711ΔAU; Fig. 3, gene C). This mutant exhibits similar kinetics to the 3′ end replacement mutant (Fig. 3, compare lanes 9–12 with 1–4). In contrast, deletion of a 543-nucleotide *Nae*I + *Bcl*I fragment of the 3′ untranslated region has essentially no effect on mRNA turnover, although perhaps increasing turnover rate slightly (Fig. 3, gene E; lanes 17–20). Duplication of this region has a similar effect (Fig. 3, gene D; lanes 13–16). These results suggest that the AU-rich sequence at the mRNA 3′ end is specifically involved in c-*fos* mRNA degradation and that proximity of the sequence to the protein coding region is not strictly required for its function. However, it is clear that deletion of the AU-rich sequences does not completely stabilize c-*fos*^{H} RNA.

We next tested whether the de-adenylation process is affected by deletion of the 3′ AU-rich sequences implicated in c-*fos* mRNA destabilization. We generated pools of mouse NIH3T3 cell lines containing either the normal c-*fos*^{H} gene pF711 or its 3′ ΔAU derivative pF711.ΔAU by cotransformation of these plasmids with plasmid pSV2neo. In contrast to transiently transfected genes, the stably transfected wild-type c-*fos*^{H} genes in these cells exhibit kinetics of mRNA induction, poly(A) tail removal and mRNA turnover that are identical to those of the endogenous murine gene (Fig. 4, lanes 1–7, lower panel; compare with Fig. 1, lanes 1–6). In the case of cells stably transfected with the 3′ ΔAU mutant gene, poly(A) shortening is both slower and apparently more processive than with the wild-type gene (Fig. 4, compare lanes 8–14 with 1–7); at present we do not know what determines the residual rate of poly(A) shortening seen in this mutant. The mutant RNA is substantially more stable than wild-type c-*fos* mRNA, with appreciable quantities persisting throughout the time course. However, degradation of 3′ ΔAU mutant mRNA is still dependent on ongoing translation, as this RNA is stable in the presence of cycloheximide (data not shown).

A number of previous observations have suggested a relation between poly(A) and mRNA degradation. Shortening of poly(A) with age, reminiscent of mRNA 'ticketing'[13] has been observed in bulk HeLa cell RNA[14,15] and in several specific cellular RNAs[16–18]; a correlation between poly(A) length and mRNA stability is observed in some[19–21] but not all[22,23] mRNAs. De-adenylated globin mRNA is unstable in microinjected frog oocytes[24], and de-adenylated mRNAs can be stabilized by polyadenylation[12,25]. Our results show that the 3′ AU-rich sequences present in shortlived mRNAs, such as c-*fos*[1–3], granulocyte/macrophage colony stimulating factor[11] and c-*myc*[6,26], act to direct rapid shortening of the 3′ poly(A) in a translation-dependent manner. The resulting de-adenylated (or oligoadenylated) RNA then forms a labile substrate for further degradation; by analogy with c-*myc* RNA this might occur by endonucleolytic cleavage

at the AU-rich sequences themselves[6]. Because the c-*fos* mRNA is relatively stable until the poly(A) tail is removed, the life of the mRNA is essentially determined by the rate of poly(A) shortening. Interestingly, many of the unstable cellular RNAs induced by growth factor stimulation exhibit such apparently two-stage kinetics of mRNA turnover[27,28]. It has been proposed that AU-rich sequences destabilize mRNAs by acting as a 'sink' for poly(A) binding proteins[6]. From our data, we prefer the idea that the poly(A) tail and 3' AU-rich sequences are basepaired and that a polysome-associated nuclease cleaves at the mismatched regions. The rapidity with which the c-*fos* poly(A) length becomes heterogeneous suggests that c-fos poly(A) shortening may occur by random endonucleolytic cleavage. We speculate that the frequency of mismatches within the basepaired region, the length of the AU-rich region itself, and its distance from the site of polyadenylation will all influence the rate of poly(A) tail shortening and hence the effective life of the mRNA: the c-*fos* 3' ΔAU mutant will be a useful gene with which both to test these ideas and to investigate other *cis* acting determinants of mRNA stability.

We thank Andy Newman and Andrew Smith for advice on *in vitro* mutagenesis and Neo transformation respectively, David Bentley and Hugh Pelham for helpful comments on the manuscript, and Sydney Brenner for arranging a DuPont studentship for T. W. This work was funded by the UK MRC.

Received 30 August; accepted 20 October 1988.

1. Greenberg, M. E. & Ziff, E. B. *Nature* 311, 433-438 (1984).
2. Kruijer, W., Cooper, J. A., Hunter, T. & Verma, I. M. *Nature* 312, 711-716 (1984).
3. Muller, R., Bravo, R., Burckhardt, J. & Curran, T. *Nature* 312, 716-720 (1984).
4. Treisman, R. H. *Cell* 42, 889-902 (1985).
5. Mitchell, R. L., Henning-Chubb, C., Huberman, E. & Verma, I. M. *Cell* 45, 567-574 (1986).
6. Brewer, G. & Ross, J. *Molec. cell. Biol.* 8, 1697-1708 (1988).
7. Fort, P. *et al. Nucleic. Acids Res.* 15, 5567-5667 (1987).
8. Rahmsdorf, H-J. *et al. Nucleic. Acids Res.* 15, 1643-1649 (1987).
9. Miller, A. D., Curran, T. & Verma, . M. *Cell* 36, 51-60 (1984).
10. Meijlink, F. & Verma, I. M. *Proc. natn. Acad. Sci. U.S.A.* 82, 4987-4991 (1985).
11. Shaw, G. & Kamen, R. *Cell* 46, 659-667 (1986).
12. Graves, R. F., Pandey, N. B., Chodchoy, N. & Marzluff, W. F. *Cell* 48, 615-626 (1987).
13. Sussman, M. *Nature* 225, 1245-1246 (1970).
14. Sheiness, D., Puckett, L. & Darnell, J. E. *Proc. natn. Acad. Sci. U.S.A.* 72, 1077-1081 (1975).
15. Sheiness, D. & Darnell, J. E. *Nature* 241, 265-268 (1973).
16. Merkel, C. G., Kwan, S-P. & Lingrel, J. B. *J. biol. Chem.* 250, 3725-3728 (1975).
17. Medford, R. M., Wydro, R. M., Nguyen, H. T. & Nadal-Ginard, B. *Proc. natn. Acad. Sci. U.S.A.* 77, 5749-5753 (1980).
18. Mercer, J. F. B. & Wake, S. A. *Nucleic Acids Res.* 13, 7929-7943 (1985).
19. Wilson, M. C., Sawicki, S. G., White, P. A. & Darnell, J. E. *J. molec. Biol.* 126, 23-36 (1978).
20. Zeevi, M., Nevins, J. & Darnell, J. E. *Molec. cell. Biol.* 7, 517-525 (1982).
21. Paek, I. & Axel, R. *Molec. cell. Biol.* 7, 1496-1507 (1987).
22. Deshpande, A. K., Chatterjee, B. & Roy, A. K. *J. biol. Chem.* 254, 8937-8942 (1979).
23. Muschel, R., Khoury, G. & Reid, L. M. *Molec. cell. Biol.* 6, 337-341 (1986).
24. Marbaix, G. *et al. Proc. natn. Acad. Sci. U.S.A.* 72, 3065-3067 (1975).
25. Huez, G. *et al. Eur. J. Biochem.* 59, 589-592 (1975).
26. Dani, C. *et al. Proc. natn. Acad. Sci. U.S.A.* 81, 7046-7050 (1984).
27. Lau, L. F. & Nathans, D. *Proc. natn. Acad. Sci. U.S.A.* 84, 1182-1186 (1987).
28. Almendral, J. M. *et al. Molec. cell. Biol.* 8, 2140-2148 (1988).
29. Van Beveren, C., van Straaten, F., Curran, T., Muller, R. & Verma, I. M. *Cell* 32, 1241-1255 (1983).
30. Van Straaten F., van Beveren, C., Curran, T. & Verma, I. M. *Proc. natn. Acad. Sci. U.S.A.* 80, 3183-3187 (1983).
31. Southern, P. & Berg, P. *J. molec. appl. Genet.* 1, 327-337 (1982).

Circulation of water within wheat grain revealed by nuclear magnetic resonance micro-imaging

C. F. Jenner*, Y. Xia†, C. D. Eccles† & P. T. Callaghan†

* Department of Plant Physiology, Waite Agricultural Research Institute, The University of Adelaide, Glen Osmond, South Australia, 5064, Australia
† Department of Physics and Biophysics, Massey University, Palmerston North, New Zealand

Observation of water movement *in situ* is difficult and very few methods are available for measuring directly the motion of water. Movement of solutes or suspended particles is not a reliable guide and the use of radioactive or heavy water is limited to a few applications. Thus, although much has been inferred about the mechanism of water movement through comparatively lengthy pathways[1], less is known for the shorter and more tortuous pathways within and between cells. Still more challenging is the investigation of water motion within structurally complex organs of small dimensions such as the fruits and seeds of plants, some of which behave (for water) as practically closed systems. We have observed longitudinally oriented bulk flow of water in developing grains of wheat using a pulsed gradient spin echo nuclear magnetic resonance technique combined with microscale imaging. Movement of water is associated with import of nutrients by the grain but is on too large a scale to be due to phloem transport alone. The flow observed could be associated with unloading and/or transport of nutrients in the vicinity of the vascular system. This is the first report of the observation *in vivo* of water movement on a sub-millimetre scale by non-invasive methods in any biological system.

Modern developments in nuclear magnetic resonance (NMR) spectroscopy involving pulsed gradient spin echo (PGSE) techniques combined with imaging methods offer the greatest promise as a means of non-invasively observing the movement of water *in situ* on a millisecond timescale. In NMR imaging, the nuclear spins in a molecule of interest (for example protons in water molecules) are given a spatial tag by acquiring the NMR precession signal in the presence of a magnetic field gradient. Refinements in methodology[2] have provided the means of imaging water proton density at a microscopic transverse resolution of around 25 μm in a 1-mm slice thickness[3]. PGSE is a well-known variant of the NMR method which involves the formation of a spin echo using two field-gradient pulses separated by a 180° radiofrequency (r.f.) pulse[4]. The position-dependent phase shifts resulting from these pulsed gradients are mutually compensating provided that the nuclear spins remain stationary over the timescale Δ between the gradient pulses. In the event of diffusive motion the pulsed gradients cause echo attenuation, an effect which has been widely exploited in the measurement of molecular self-diffusion[5]. When there is coherent motion, the echo suffers a phase shift, an effect which can in principle be used to measure molecular velocity.

The PGSE and imaging methods may be combined by applying the imaging field gradients to the modulated echo[3]. By independent variation of both the imaging and the PGSE gradients, the spatial positions and the translational motions of nuclear spins can be revealed. The simplest application would involve the observation of attenuation contrast in the image as a result of molecular self-diffusion. A more sophisticated approach uses Fourier analysis of the image modulation as the PGSE gradient pulses are varied in magnitude. Recently it has been shown that this technique enables static spin maps and dynamic nuclear spin displacement profiles to be measured at microscopic resolution in the same experiment[6]. In an earlier study we used simple PGSE contrast methods to detect the regional variation in the diffusion of water in the transverse plane of the developing wheat grain[7] with a transverse resolution of about 150 μm. Diffusive motion of water was hindered, especially in the endosperm but less so in regions through which nutrients travel on their way through the grain and into the endosperm.

Transport of nutrients within the grain[8] involves mass flow of solution acropetally along the vascular bundles of the furrow accompanied by the re-circulation of much, if not all, of the water within the grain. The combined static/dynamic NMR microscopy method[6] has made it possible to measure simultaneously the motion of water attributable to bulk flow and to